JOURNAL OF AGRICULTURAL AND FOOD CHEMISTRY

Effects of Droplet Crystallization and Melting on the Aroma Release Properties of a Model Oil-in-Water Emulsion

SUPRATIM GHOSH, DEVIN G. PETERSON, AND JOHN N. COUPLAND*

Department of Food Science, The Pennsylvania State University, 103 Borland Lab, University Park, Pennsylvania 16802

Aroma compounds partition between the dispersed and the continuous phases in emulsions, and phase transitions in the lipid droplets profoundly affect the position of the equilibrium. In the present study, the release of ethyl butyrate, ethyl pentanoate, ethyl heptanoate, and ethyl octanoate from a series of sodium caseinate-stabilized, *n*-eicosane emulsions was investigated as a function of solid and liquid lipid droplet concentration. For all compounds, headspace volatile concentrations above the solid droplet emulsions were higher than those above the liquid droplet emulsions. The interaction with liquid droplets could be modeled in terms of volume-weighted bulk partition coefficients while the more nonpolar volatiles bound to the surface of solid lipid droplets. The amount of volatiles bound to solid surfaces increased with aqueous concentration up to a critical point and then rapidly increased. The critical point corresponds to the dissolution of the solid lipid in a phase of adsorbed volatile. The binding of volatiles to both solid and liquid eicosane droplets is reversible.

KEYWORDS: Aroma release; lipid crystallization; surface adsorption; emulsion

INTRODUCTION

Flavor is one of the most important factors in determining food choice (*1*). The perception of food flavor is dependent on many parameters and includes stimuli from both volatile and nonvolatile components (*2*). The perceived aroma, unquestionably a key component of food flavor, not only depends on the type and concentration of volatile compounds present in the headspace (HS) above the food and how they interact with appropriate sensory receptors in the nose and mouth (*3*, *4*) but also is influenced by the presence of certain food components (e.g., sweetener) and food textures (*5*, *6*). Defining the mechanisms that govern the HS volatile concentration are therefore key to understanding food flavor and ultimately a function of the absolute amount of each volatile compound present in the food and by their ability to partition into the gas phase.

Partitioning can be described thermodynamically as the ratio of activities of the compound in each phase. Because the concentration of aroma molecules is typically very low, the activity coefficients are approximately unity and activity can be replaced by concentration. Thus, the partition coefficient for a volatile into the HS above a simple liquid food can be expressed as (*7*):

$$K_{gl} = \frac{c_g}{c_l} \quad (1)$$

where c_g and c_l are the concentrations of the aroma compound in the HS and liquid phase, respectively. However, most foods themselves consist of more than one phase and we need to also consider partitioning of aroma molecules within the food. An oil−water partition coefficient is similarly expressed as the ratio of concentrations of the compound of interest in the oil phase (c_o) to that in the aqueous phase (c_w):

$$K_{ow} = \frac{c_o}{c_w} \quad (2)$$

So, for a simple food emulsion consisting of an oil and an aqueous phase in contact with the air, the overall distribution of volatile molecules would be (*8*):

$$\frac{1}{K_{ge}} = \frac{\phi_o}{K_{go}} + \frac{\phi_w}{K_{gw}} \quad (3)$$

where K_{ge} is the overall gas−emulsion partition coefficient, ϕ_o and ϕ_w are the volume fraction of lipid phase and aqueous phase in the emulsion, and K_{go} and K_{gw} are the individual gas−oil and gas−water partition coefficients, respectively. Clearly from eq 3, increased lipid content will reduce the volatility of

Table 1. Mean Droplet Size (d_{32}) of Emulsions under Different Homogenization Conditions

homogenization pressure (MPa)	homogenization time (min)	emulsion mean droplet size (d_{32}) (μm)
14 ± 1	3	0.97 ± 0.12
25 ± 1	8	0.44 ± 0.05
59 ± 1	8	0.28 ± 0.02

* To whom correspondence should be addressed. Tel: 814-865-2636. Fax: 814-863-6132. E-mail: coupland@psu.edu.

10.1021/jf052262w CCC: $33.50
Published on Web 02/04/2006

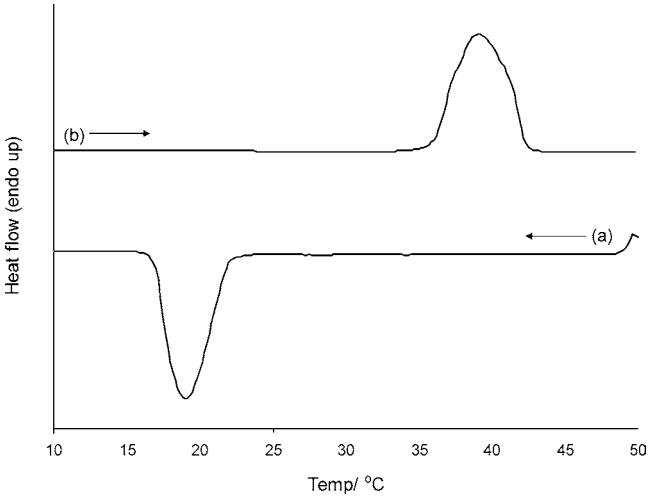

Figure 1. Thermogram of *n*-eicosane emulsion during (**a**) cooling and (**b**) heating. The emulsion was 40 wt % lipid stabilized with 2 wt % sodium caseinate solution and was cooled and heated at 5 °C min^{-1}.

hydrophobic volatile molecules more than the volatility of hydrophilic volatile molecules.

This approach has been used to describe the HS volatile concentration in equilibrium with a food sample (*9*−*12*), and in many cases, emulsions are used as model systems (*13*−*16*). Several workers have studied flavor release from emulsions as influenced by the properties of the flavor molecules (*17*) and their binding to the interface (*18*, *19*) and several other components (*20*−*22*) and by the physical properties of the component phases (*23*). However, most of these studies involve exclusively liquid oil and the effect of fat crystallization on volatile partitioning is less well-understood.

McNulty and Karel (*10*) investigated the release rates of *n*-alcohols (C-6, C-8) from a bulk lipid phase as a function of solid fat index and concluded that flavor diffusion primarily occurred in the liquid portion of the lipid. Maier (*24*) showed that solid triglycerides bind much less aroma compounds than liquid triglycerides and proposed that sorption to solid fat occurs at the crystal surface. Roberts et al. (*25*) studied the effects of the solid fat content of lipid droplets on the amount of flavor release from milk-based emulsions. A significant increase in the HS concentration of nonpolar flavor compounds was observed with an increase in solid fat content, whereas polar flavor compounds showed no significant change. It was concluded that only the liquid lipids could absorb nonpolar flavor compounds; hence, fat crystallization would reduce the effective lipid content. Similar observations were also obtained by Dubois, Sergent, and Voilley (*26*) who studied effects of fat type on the release of aroma compounds from a model cheese. The authors found that volatility of hydrophobic diallyl sulfide decreased by 20% in the presence of liquid tributyrin as compared to milk fat with 15% solid triglycerides while the volatility of the more hydrophilic compound diacetyl was not affected by the presence of solid fat. However, other workers (*27*, *28*) showed that the partitioning of flavors was not affected by crystallization of the lipid phase of emulsions.

In the present work, the partitioning behavior of an homologous series of volatile aroma compounds was measured for a series of both model emulsions containing either solid or liquid droplets as a function of lipid content and particle size. Eicosane was chosen as the model lipid for these studies, as its deep supercooling in the emulsified state allowed us to measure the partitioning behavior of solid and liquid droplets at the same temperature (see below for details). It should be noted that significant chemical differences exist between eicosane, an *n*-alkane, and other food oils (mixture of triacylglycerols). However, because of their similar physical properties, eicosane was considered an acceptable model. The volume partitioning approach (eq 3) was used as a basis for understanding the phase behavior of the volatiles, but this was further modified to show the effect of binding at the surface of the solid lipid droplets. A time−series experiment of volatile partitioning in HS was also performed to confirm the thermodynamic reversibility of volatile binding by solid lipid.

MATERIALS AND MATERIALS

Materials. Eicosane and hexadecane were purchased from Fisher Scientific (Springfield, NJ). Sodium caseinate, all four aroma compounds (ethyl butanoate, EB; ethyl pentanoate, EP; ethyl heptanoate, EH; and ethyl octanoate, EO), and ethyl alcohol (high-performance liquid chromatography grade) were obtained from the Sigma Chemical Co. (St. Louis, MO).

Emulsion Preparation. The model system selected for this study was a fine dispersion of *n*-eicosane droplets stabilized with sodium caseinate. Emulsions were prepared by mixing *n*-eicosane (40% w/w) with sodium caseinate solution (2% w/w) containing 0.02% (w/w) thimerosal as an antibacterial agent (Sigma Chemical Co.). An initial oil-in-water emulsion premix was made using a high-speed blender (Brinkmann Polytron, Brinkmann Instruments Inc., Westbury, NY) for 30 s. The coarse emulsions were then recirculated through a twin-stage valve homogenizer (Niro Soavi Panda, GEA Niro Soavi, Hudson, WI) for several minutes at different pressures (15−60 MPa) to achieve multiple passes through the valves. Emulsions were prepared hot (>40 °C) to ensure that the lipid was liquid. The particle size distribution of the emulsions was characterized by laser diffraction particle sizing (Horiba LA 920, Irvine, CA) using a relative refractive index of 1.15. The emulsions were stored at 40 °C prior to use and were stable over several weeks (no change in particle size and appearance).

Thermal Analysis. The crystallization and melting behavior of bulk and emulsified eicosane were determined using a differential scanning calorimeter (DSC; Perkin-Elmer DSC-7, Norwalk, CT). The instrument was calibrated against indium. Aliquots of sample (∼15 mg) were temperature cycled in the DSC from 50 to 10 °C to 50 °C at 5 °C min^{-1}, and the crystallization and melting points were taken from the onset temperature of peaks on the thermogram using Pyris data analysis software (version 3.52, Perkin-Elmer Corp.). All analyses were conducted in triplicate.

Addition of Aroma Compounds to Emulsions. The relative concentrations of four aroma compounds were selected so that after partitioning with an emulsion each compound would give a readily quantifiable peak from 1 mL of HS sample on a gas chromatogram. Four aroma compounds, EB, EP, EH, and EO, were mixed in a volumetric ratio of 1:2:20:20 and diluted in an equal volume of ethyl alcohol.

The initial 40% (w/w) emulsion was diluted with deionized water to produce a series of samples with different oil contents. Aliquots (2 mL) of each emulsion were added to 20 mL HS vials (MicroLiter Analytical Supplies, Inc., Suwanee, GA), which were temperature-cycled to produce either wholly solid or wholly liquid droplets (see below for more discussion of the crystallization behavior of emulsified *n*-eicosane and the temperature cycling protocol). Stock aroma solution (860 μL/L of emulsion) was added to the emulsions so that the final concentrations (μL/L) of aroma compounds in the emulsion were EB, 10; EP, 20; EH, 200; and EO, 200. The vials were sealed with poly(tetrafluoroethylene)/butyl rubber septa (MicroLiter Analytical Supplies, Inc.) and equilibrated at 30 °C for at least 1 h prior to analysis. Note that work reported below shows that the HS concentration of volatiles above both solid and liquid emulsions is independent of time for periods between 1 h and over a week, suggesting that this equilibration time is sufficient.

HS Analysis by Gas Chromatograph (GC). After equilibration, a sample of the HS (1 mL) was withdrawn using an autosampler

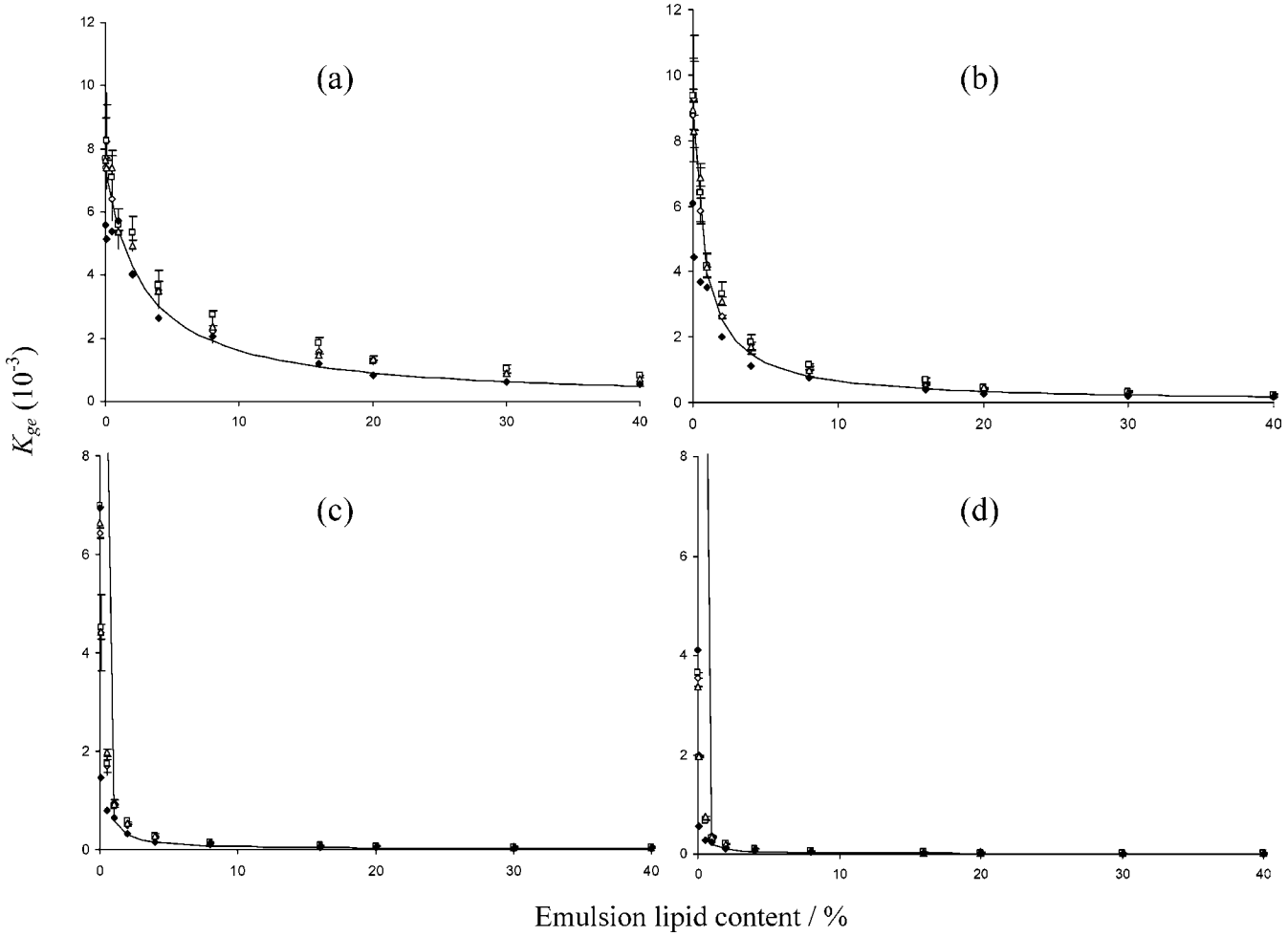

Figure 2. Gas–emulsion partition coefficient (K_{ge}) of aroma compounds as a function of lipid content of emulsions with liquid lipid (**a**) EB, (**b**) EP, (**c**) EH, and (**d**) EO. Results for emulsions with different particle sizes (d_{32}) 0.97 (◇), 0.44 (□), and 0.28 μm (△) are shown along with bulk lipid and water mixtures (◆). Predicted lines (from eq 3) are shown for each compound alongside the experimental data points. Note the difference in scales for K_{ge} values used in the different plots.

(Combi-Pal, CTC Analytics, Carrboro, NC) and injected into a gas chromatograph (Agilent 6890, Agilent Technologies, Palo Alto, CA) equipped with a DB-5 capillary column (30 m × 0.32 mm i.d. with a 1 μm film thickness) and a flame ionization detector. The operating conditions were as follows: The sample was injected in splitless mode (purge value on at 1 min); the inlet temperature was 200 °C, the detector temperature was 250 °C, the oven program was 30 °C for 1 min, then increased at 35 °C min^{-1} from 30 to 200 °C, and held for 2 min; and the carrier constant flow rate was 2.0 mL min^{-1} (H_2). Static HS concentrations were determined from peak areas using a standard calibration curve ($R^2 = 0.99$). All measurements were expressed as the mean and standard deviation of at least two full experimental replicates.

Gas−water and gas−oil partition coefficients for each aroma compounds were determined using the same HS GC protocol as above. Mixed aroma stock [12.5−800 μL/L (v/v)] was added to HS vials containing 2 mL of either the water or the lipid. The vials were sealed and equilibrated at 30 °C for at least 1 h before measuring the HS volatile concentrations by GC.

RESULTS AND DISCUSSION

The emulsions were reasonably monodispersed with approximately log-normal distributions (standard deviation of distributionm ~0.19 ± 0.2). The particle size could be controlled by varying the homogenization conditions (**Table 1**).

Crystallization of Eicosane. A DSC thermogram of emulsified eicosane (40% w/w) is shown in **Figure 1**. Both the bulk eicosane (data not shown) and the emulsified eicosane droplets melted at 36 °C, but while the bulk lipid crystallized at 35 °C (i.e., 1 °C of supercooling), emulsified eicosane droplets crystallized at 22 °C (i.e., 13 °C of supercooling). Deep supercooling is characteristic of emulsified alkanes (*29*) and is thought to be due to a homogeneous nucleation mechanism (*30*). The supercooled eicosane is very stable, and it was possible to maintain liquid droplets at 30 °C for several weeks without measurable crystallization. Therefore, by adjusting the temperature history of the eicosane emulsion, it was possible to produce either solid or liquid lipid droplets of the same chemical composition at the same temperature (30 °C): (i) solid lipid droplets, cool from storage temperature (40 °C) to 10 °C to induce crystallization and then reheat to the experimental temperature (30 °C); (ii) liquid lipid droplets, cool from the storage temperature (40 °C) to the experimental temperature (30 °C). Note that while an emulsion is defined as a fine dispersion of one liquid in a second, largely immiscible liquid (*13*), we also use the term for the solid droplets used in this study.

Determination of Partition Coefficients. Solutions of the aroma compounds cocktail were prepared in water or lipid, and the HS volatile concentrations were measured as a function of solution concentration. The HS concentration initially increased linearly with solution concentration, but for EH and EO in water, the HS concentrations reached a plateau value at the aqueous

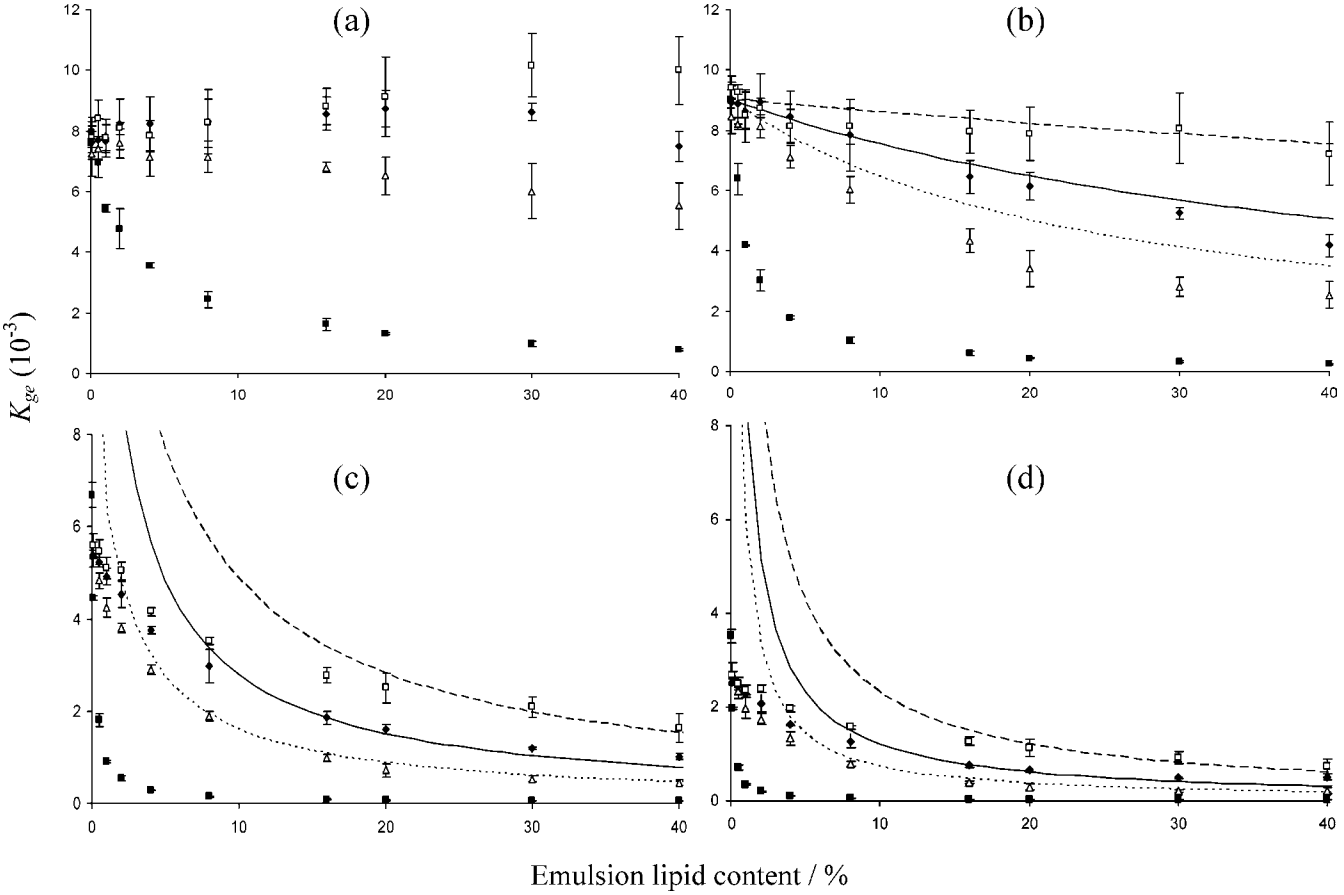

Figure 3. Gas–emulsion partition coefficient (K_{ge}) of aroma compounds as a function of lipid content of emulsions with solid lipid (**a**) EB, (**b**) EP, (**c**) EH, and (**d**) EO. Results for emulsions with different particle sizes (d_{32}) 0.97 (□), 0.44 (◆), and 0.28 μm (△) are shown along with the model predicted lines (from eq 4) for three different particle sizes: 0.97 (– – –), 0.44 (—), and 0.28 μm (- - -). For comparison, the average values from the corresponding liquid lipid emulsion (■) (from eq 5) are also shown. Note the difference in scales for K_{ge} values used in the different plots.

Table 2. Air–Water (K_{aw}), Air–Oil (K_{ao}), and Oil–Water (K_{ow}) Partition Coefficients and Surface Binding Coefficients (K_{iw}*) of Aroma Compounds[a]

flavor compounds	K_{aw}	K_{ao}	K_{ow}	K_{iw}* (m)
EB	7.35×10^{-3}	2.0×10^{-4}	36.75	
EP	9.02×10^{-3}	7.0×10^{-5}	128.86	2.2×10^{-7}
EH	1.82×10^{-2}	6.0×10^{-6}	3033.33	4.3×10^{-3}
EO	2.67×10^{-2}	2.0×10^{-6}	13350	1.6×10^{-5}

[a] Unit of K_{iw}* is expressed as meters.

solubility limit and further additions of volatiles lead to the formation of a separate surface phase on the water. The partition coefficients were determined from the slope of the linear portion of the plot (data not shown), and the aroma concentrations used elsewhere in this study were all within the linear region. The gas−oil (K_{go}) and gas−water (K_{gw}) partition coefficients were determined against the lipid ($R^2 = 0.91$) or water ($R^2 = 0.97$) phase concentration while the oil−water partition coefficient (K_{ow}) was calculated from the ratio of gas−water to gas−oil partition coefficients (**Table 2**).

It should be mentioned that as bulk eicosane does not show a large supercooling and is solid at the temperature used for the experiments (30 °C), *n*-hexadecane was selected as an analogue for gas−liquid lipid partition coefficient determination. The physical properties of the two liquid alkanes are very similar (*31*), and it is expected that their partitioning behaviors will also be similar. Indeed, in an experiment to compare the effect of two alkanes, the HS volatile concentration from both liquid eicosane and hexadecane emulsions was measured with different lipid contents and no significant difference in the results was found (data not shown).

Partitioning Behavior of Liquid Lipid Emulsions. Aliquots of the aroma compounds mixture were equilibrated with liquid eicosane emulsions, and the HS concentration was measured as a function of emulsion lipid content and emulsion particle size. Similar experiments were also conducted with unhomogenized mixtures of bulk lipid (again hexadecane was used in place of eicosane in the bulk studies to ensure the lipid remained liquid) and water with the same compositions as the emulsions. Gas−emulsion partition coefficient (K_{ge}) values were calculated from the HS concentration data for each emulsion and for the bulk mixture and are plotted as a function of lipid concentration in **Figure 2**. These data were modeled using eq 3 and the partition coefficients established for the pure bulk phases reported in **Table 2**. In applying this model, it was assumed that the aqueous caseinate−volatile interactions are negligible, and indeed, in preliminary work, it was observed that repeating the experiment with different concentrations of aqueous caseinate (0.2 and 2% w/w) did not affect the results.

The partition coefficient of all volatiles decreased with lipid content, but there was no effect of emulsion particle size. The unhomogenized samples behaved similarly to the homogenized samples (**Figure 2**). As anticipated, the effect of lipid content was greater for the nonpolar volatiles (EH and EO) than for the polar compounds (EB and EP) due to their lower oil−water

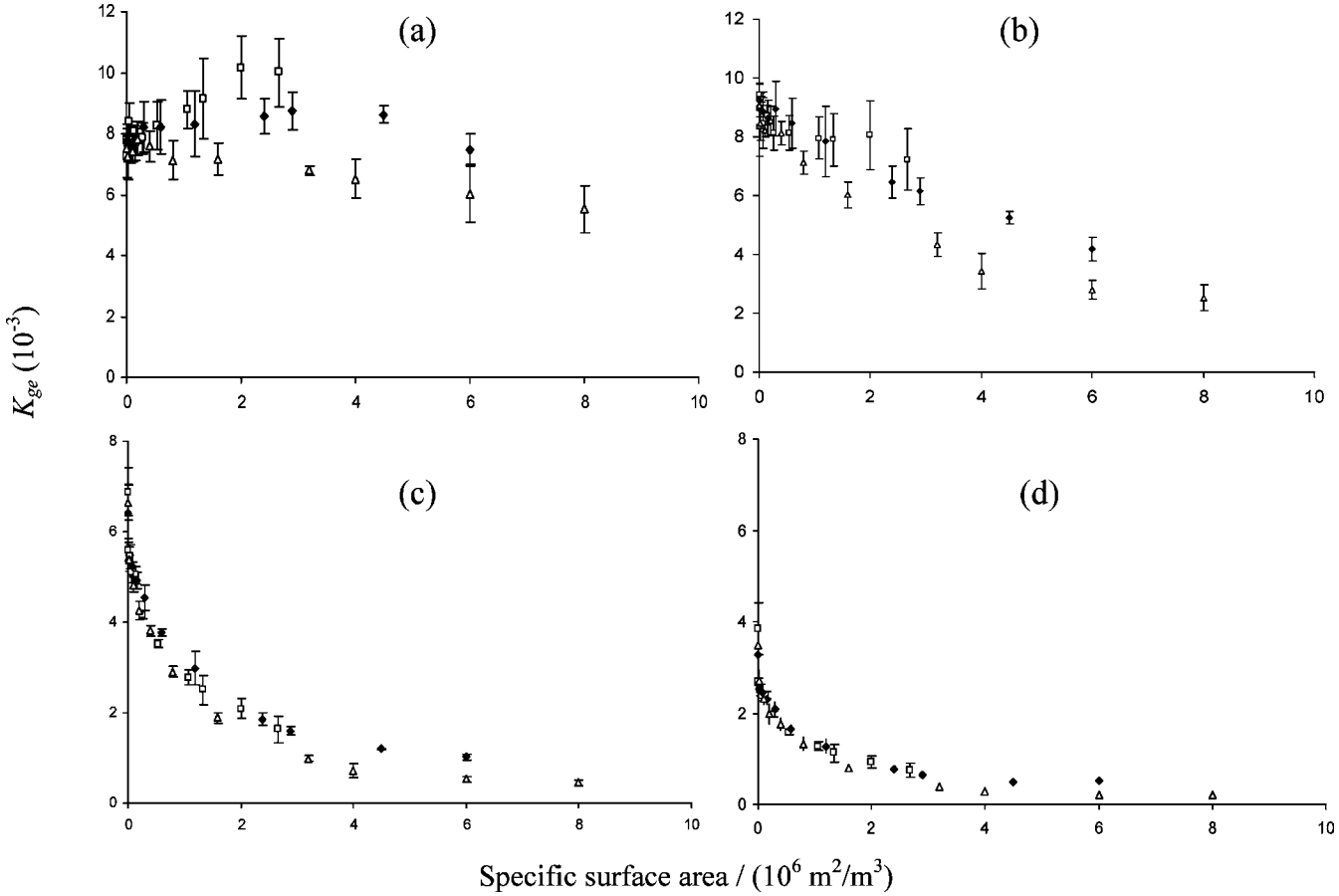

Figure 4. Gas–emulsion partition coefficient (K_{ge}) of aroma compounds as a function of specific surface area of lipid droplets of emulsions with solid lipid (**a**) EB, (**b**) EP, (**c**) EH, and (**d**) EO. The particle sizes (d_{32}) of emulsions with solid lipid droplets were 0.97 (□), 0.44 (◆), and 0.28 μm (△).

partition coefficients. The model based on the independent measurements of bulk partitioning behavior (eq 3) agreed reasonably with the experimental results for the emulsions. In the next series of experiments, these studies were repeated using solid droplets.

Partitioning Behavior of Solid Lipid Emulsions. The HS concentrations of the four volatile compounds were measured as a function of lipid content for emulsions of solid eicosane droplets, and the gas−emulsion partition coefficient (K_{ge}) values were calculated from the HS concentration data as before (**Figure 3**). To allow comparison, average values for liquid lipid droplets measured above are shown alongside these data. (Note that the plots for EH and EO were plotted in a different scale to show the effects of droplet particle size on the K_{ge} values.) The gas−emulsion partition coefficients (K_{ge}) for solid lipid emulsions were higher than those of liquid lipid emulsions for all four aroma compounds. Moreover, the K_{ge} values for EH and EO decreased monotonically with lipid concentration, suggesting an association of aroma molecules with solid lipid droplets.

Notably, the smaller solid particles had a bigger effect on K_{ge} than the larger ones suggesting that the interaction may depend on droplet surface area rather than volume. The specific surface area of the solid emulsions was calculated from

$$A_s = \frac{6\phi}{d_{32}} \tag{4}$$

(where ϕ is the lipid volume fraction and d_{32} is the volume−surface mean diameter) and used to replot the data from **Figure 3** (as **Figure 4**). Plotted in terms of interfacial area, K_{ge} is independent of particle size, supporting our hypothesis that the bound volatiles are adsorbed at the droplet surface. The effect is more significant for the higher molecular weight volatiles (more hydrophobic) EH and EO than EB and EP indicating that polarity of aroma compounds influences their surface adsorption ability. The term binding is used here to describe any physical association of aroma compounds (adsorption as well as absorption) to lipid phase.

This type of surface adsorption was proposed by Maier (*24*) who showed that although the amount of volatiles bound by solid trilaurin was much less than that bound by liquid tributyrin, the initial rate of sorption was much faster for the solid lipid, indicating that the process occurred at the surface. However, this is in contrast with the findings of McNulty et al. (*10*) and Roberts et al. (*25*) who proposed that only liquid oil could bind aroma compounds. One reason for the apparent disparity between the present work and the Roberts et al. (*25*) paper may be due to the relatively low-fat emulsions used in their experimental design (1.38 wt %/vol) and consequently less interfacial area to adsorb aroma compounds. Also, a partially crystalline lipid was used in Roberts et al. (*25*) study in comparison with complete solid lipid used in the present work.

To model aroma release from emulsion with solid lipid droplets, an additional term is required to account for surface binding in eq 3 (*13*):

$$\frac{1}{K_{ge}} = \frac{\phi_o}{K_{ow}} + \frac{\phi_w}{K_{gw}} + \frac{K_{iw}^* \cdot A_s}{K_{gw}} \tag{5}$$

where A_s is the interfacial area per unit volume of emulsion

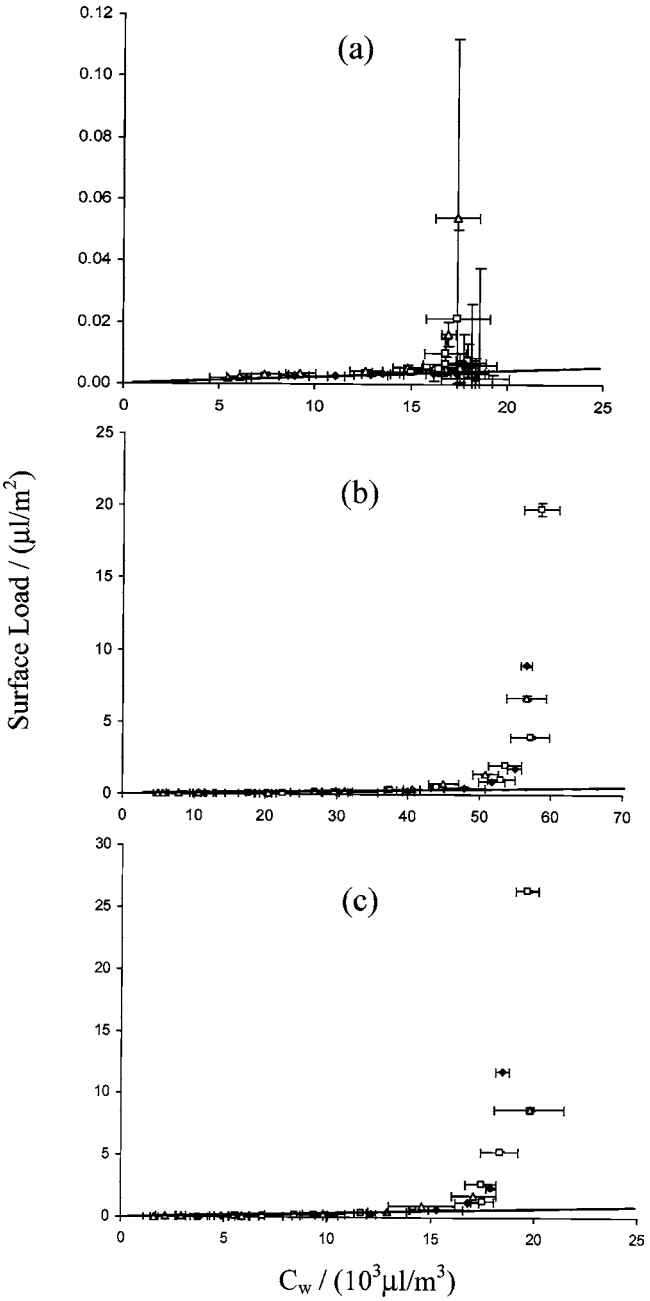

Figure 5. Surface adsorption isotherm of aroma compounds (**a**) EP, (**b**) EH, and (**c**) EO at 30 °C. Values of surface load (volume of aroma compounds adsorbed per unit area of droplet surface) are plotted as a function of aqueous phase aroma concentration. Results for emulsions with solid lipid particle sizes (d_{32}) 0.97 (□), 0.44 (◆), and 0.28 μm (△) are shown along with the best fit line to the linear portion of the graph. Note the difference in scales used in the different plots.

and K_{iw}* is the apparent surface binding coefficient defined as

$$K_{iw}^* = \frac{\Gamma_i}{C_w} \quad (6)$$

where Γ_i is the surface load, i.e., volume of aroma compound per unit interfacial area (μL/m^2).

To model the binding effects of solid emulsion droplets, it was assumed that the volatiles can only interact with the surface of the crystalline lipid; thus, the first term on the right-hand side of eq 5 can be neglected.

Surface load (Γ_i) was calculated from the data shown in **Figure 4** and the air−water partition coefficient in **Table 2**

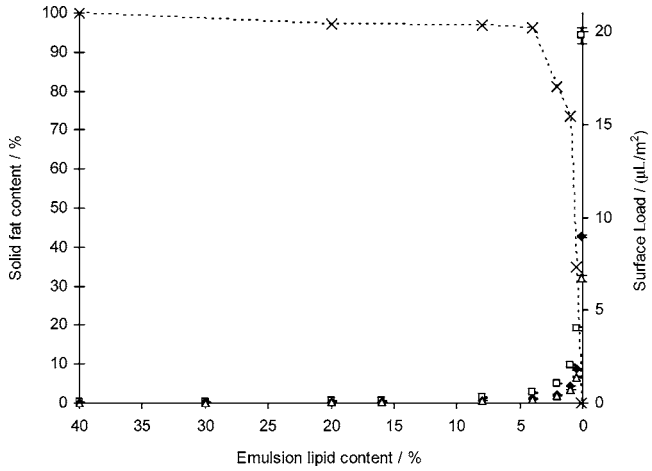

Figure 6. Calculated values of percent solid lipid in emulsions as a function of lipid content (-×-). Percent solid lipids were calculated from the difference between the melting enthalpies of lipid in emulsions (d_{32} = 0.44 μm) prepared with and without added volatiles. Surface loads of only EH were shown as a function of emulsion lipid content alongside the solid fat content data to maintain clarity. Particle sizes (d_{32}) of emulsions are 0.97 (□), 0.44 (◆), and 0.28 μm (△).

assuming that volatiles present in the HS are at equilibrium with the emulsion aqueous phase and that the total amount of aroma compounds added are distributed between the HS, the aqueous phase, and the surface of solid droplets (**Figure 5**). However, this calculation was not performed for EB, as this compound showed no measurable surface binding. The surface load increased slowly with equilibrium aqueous phase concentration (C_w) up to a critical point and then rapidly beyond that. It should be noted that the sharp increase in surface load, which occurs at a high aqueous phase concentration, corresponds to a very dilute emulsion (<1% lipid).

At low values of C_w, below the critical point, K_{iw}* was calculated from the slope of the best fit line to the linear portion of the curve (**Figure 5**) and reported in **Table 2**. However, this value is only representative below the critical point and does not account for the behavior at higher C_w. The K_{iw}* calculated in this manner was used in eq 5 to calculate the corresponding gas−emulsion partition coefficient (K_{ge}). The model-predicted K_{ge} values were plotted alongside the experimental data (**Figure 3**), and reasonable fits were seen for ϕ > ~10%. Lower lipid content emulsions have higher aqueous volatile concentrations and consequently lie beyond the critical point seen in **Figure 5** where the simple single value of K_{iw}* cannot be expected to adequately model the data. It was not possible to model the EB data by this method as adequate measurement of K_{iw}* was not obtained due to the small amount of adsorption to the solid lipid surface.

Figure 5 represents a surface adsorption isotherm for volatiles onto solid lipid droplets and bears some physical similarity to the moisture sorption isotherm of some sugars (*32*−*34*). In dry conditions, sugars adsorb small amounts of moisture roughly proportional to the humidity of the gas surrounding them, but at a critical humidity, the moisture content of the sugars rapidly increases as they dissolve in the adsorbed water. Extending the physical analogy to the current case, it seems adsorption at low values of C_w follows a simple proportionality, but at the critical value, the system suddenly changes so that the amount of adsorbed volatile increases. Our hypothesis is that the initial adsorption is of isolated volatile molecules, but at the critical level, the adsorbed molecules begin to interact to an extent that they can be treated as a separate thermodynamic phase and begin

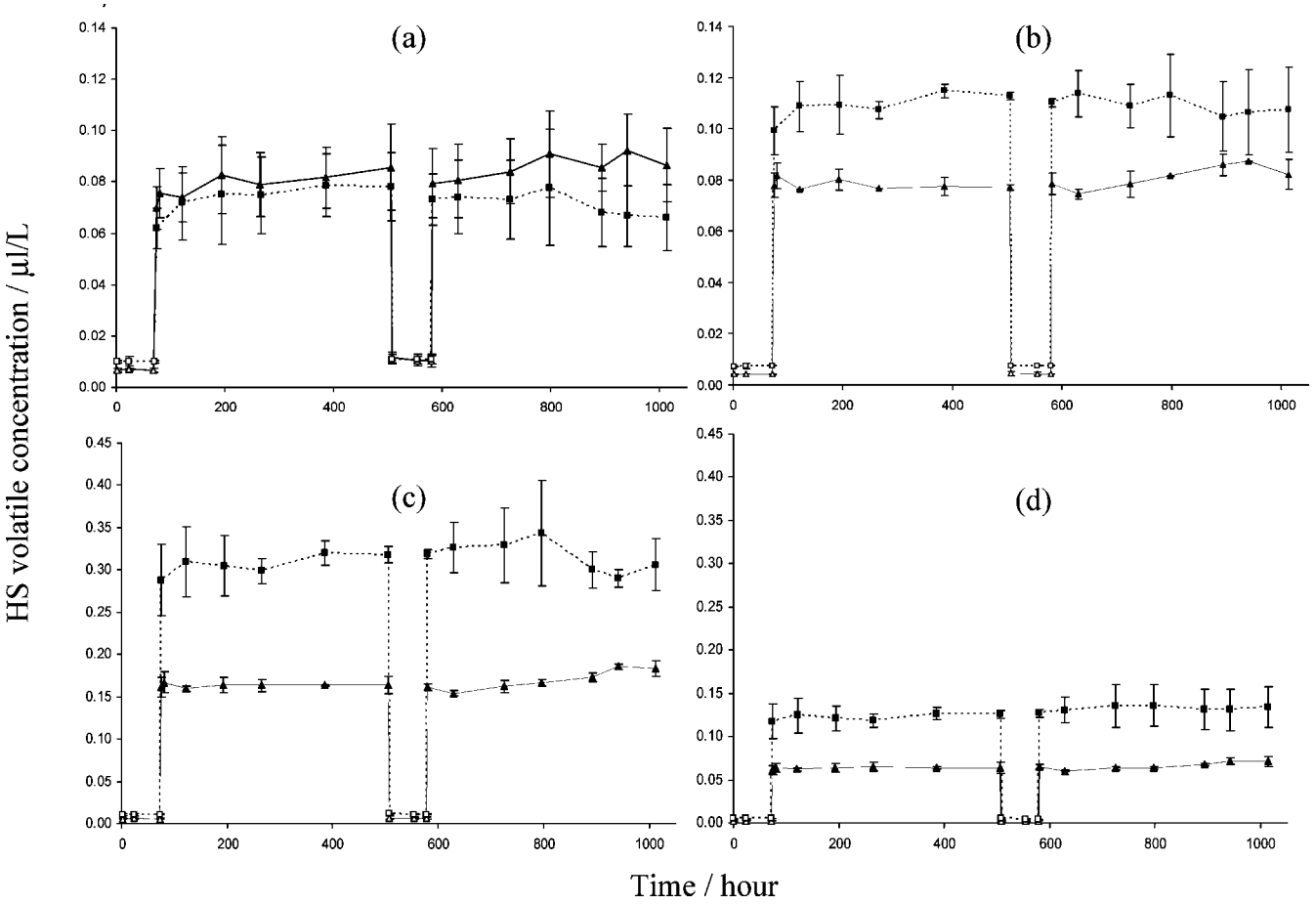

Figure 7. HS concentrations of aroma compounds at 30 °C from 40% emulsion (-▲-) and 20% emulsion (-■-) with liquid lipid (open symbol) and solid lipid (closed symbol) as a function of time: (**a**) EB, (**b**) EP, (**c**) EH, and (**d**) EO. Note the difference in scales for HS volatile concentration used in the different plots.

to dissolve the solid lipid. More volatile added will rapidly dissolve in this new phase increasing the amount bound. This seems to be true for the relatively nonpolar compounds (EO and EH) as more polar compounds have less surface affinity (EB). However, if this hypothesis is correct, dispersions of solid particles in aqueous phases with high C_w (i.e., low lipid, high added volatiles) should effectively dissolve in the aroma molecules and have no detectable crystallinity. Similar associations were seen in studies of solid lipid nanoparticles used for drug delivery by Bunjes et al. (*35*) who proposed that while a portion of the solute firmly associated with solid particle (either incorporated into crystal structure or adsorbed on surface), excess adheres as a liquid phase to the droplet surface. Westesen et al. (*36*) also found formation of liquid triglycerides at higher drug load on solid lipid nanoparticles indicating similar behavior as observed here. In the drug delivery studies, however, the drug components were added to lipid phase before homogenization, whereas in this study the aroma compounds were added after homogenization and droplet crystallization. Nevertheless, as shown below, the lipid−volatile interactions were reversible with respect to droplet crystallization and we expect a similar behavior if the volatiles were added to lipid before homogenization.

To test the hypothesis, DSC was used to measure the ratio of the melting enthalpies between emulsions prepared with and without added volatiles (only the emulsion with $d_{32} = 0.44\ \mu$m was used) and the difference between the two enthalpies was expressed as solid fat content (**Figure 6**). The surface loads of EH (from **Figure 5**) are shown along with the solid fat content data. EP and EO also follow a similar behavior as EH in **Figure 6**; however, only the data for EH were shown to maintain clarity. The particles remained crystalline for $\phi > 4\%$, but at lower lipid contents, the solid fat content rapidly decreases. This transition coincides with the critical point in the surface binding isotherm and supports our hypothesis that the crystalline droplets can be dissolved if sufficient volatile adsorbs to their surface.

Reversibility. Finally, the reversibility of the interactions between the volatiles and the solid and liquid emulsion droplets, the aqueous phase, and the HS was tested in a time−series experiment in which flavored emulsions were temperature cycled to produce alternately solid and liquid particles. The concentration of HS volatiles above samples of emulsion ($\phi =$ 20 and 40% w/w, $d_{32} = 0.44\ \mu$m) was measured at 30 °C over several days. The experiment started with liquid lipid emulsions, and at intervals, the emulsions were (i) crystallized (cooling to 10 °C) and then reheated to the analysis temperature (30 °C) before continued monitoring (now with solid lipid droplets) and (ii) melted (heating to 50 °C) once more before returning again to 30 °C (with liquid lipid droplet). Three separate vials were used for each analysis and then discarded.

The HS concentrations of all of the aroma compounds were plotted as a function of time in **Figure 7** for both 40 (w/w) and 20% (w/w) lipid emulsions. The HS concentrations of all compounds increased dramatically on droplet crystallization (74 h) as the volatiles were expelled from the solid lipid (although a smaller fraction will adsorb at the solid surface). Thereafter, the HS concentration from solid droplet emulsions was measured for several days and no significant change was observed. On

remelting (507 h), the aroma compounds were reabsorbed by liquid lipid and the HS volatile concentrations returned to the same levels as at the beginning of the experiment. Further temperature cycles were also repeatable, indicating that the lipid−volatile interactions were reversible. **Figure 7** also showed that emulsions with more solid lipids (40% w/w) had less aroma compounds in the HS because they had more solid surface for aroma adsorption. However, for the EB 40% solid lipid droplet, emulsion had a higher HS concentration than the corresponding 20% emulsion as this compound does not measurably bind to the solid surface.

The fact that the binding of volatiles was reversible suggests that the process is thermodynamically driven and, at least in this case, the compounds are not trapped in the lipid structure. This is in contrast with the results of Roberts et al. (*25*) who proposed that absorbed aroma compounds in liquid oil were entrapped by solid fat during crystallization. However, the chemical nature of the lipid used (hydrogenated palm fat) was considerably different than pure *n*-eicosane used in the present study and this could influence flavor−fat interactions considerably. In the study of controlled drug release using solid lipid nanoparticles, it was observed that while lipids forming crystals with perfect lattice lead to drug expulsion, complex lipid mixtures forming less perfect crystals can accommodate the drugs (*37*). Similarly, in the present work, *n*-eicosane crystallized in pure form (*38*) and mutually excluded all of the foreign materials present.

From this work, we conclude that (i) the interactions of volatile molecules with liquid lipid emulsions can be described in terms of a three-phase partitioning (eq 3), (ii) more nonpolar volatiles can interact with the surface of solid lipid droplets, and (iii) the binding of volatiles on solid lipid surfaces is proportional to the aqueous concentration up to a critical point then rapidly increases. The critical point corresponds to dissolution of the solid lipid in a phase of adsorbed volatile, and (iv) the binding is thermodynamically driven and is reversible.

LITERATURE CITED

(1) Roberts, D. D.; Taylor, A. J. Flavor release: A rationale for its study. In *Flavor Release*; Roberts, D. D., Taylor, A. J., Eds.; ACS Symposium Series; American Chemical Society: Washington, DC, 2000; pp 1−3.

(2) Laing, D. G.; Jinks, A. Flavour perception mechanisms. *Trends Food Sci. Technol.* **1996**, *7*, 387−389.

(3) Taylor, A. J.; Linforth, R. S. T. Flavour release in the mouth. *Trends Food Sci. Technol.* **1996**, *7*, 444−448.

(4) Overbosch, P.; Afterof, W. G. M.; Haring, P. G. M. Flavor release in the mouth. *Food Rev. Int.* **1991**, *7*, 137−184.

(5) Pionnier, E.; Nicklaus, S.; Chabanet, C.; Mioche, L.; Taylor, A. J.; Le Quere, J. L.; Salles, C. Flavor perception of a model cheese: Relationships with oral and physicochemical parameters. *Food Qual. Pref.* **2004**, *15*, 843−852.

(6) Friel, E. N.; Taylor, A. J. Effect of salivary components on volatile partitioning from solutions. *J. Agric. Food Chem.* **2001**, *49*, 3898−3905.

(7) Wedzicha, B. L. Distribution of low molucuar weight food additives in dispersed systems. In *Advances in Food Emulsions*; Dickinson, E., Stainsby, G., Eds.; Elsevier: London, United Kingdom, 1988; pp 329−371.

(8) Buttery, R. G.; Guadagni, D. G.; Ling, L. C. Flavor compounds: volatilities in vegetable oil and oil−water mixtures. Estimation of odor thresholds. *J. Agric. Food Chem.* **1973**, *21*, 198−201.

(9) McNulty, P. B.; Karel, M. Factors affecting flavor release and uptake in O/W emulsions, 1. Release and upake models. *J. Food Technol.* **1973**, *8*, 309−318.

(10) McNulty, P. B.; Karel, M. Factors affecting flavor release and uptake in O/W emulsions, 2. Stirred cell studies. *J. Food Technol.* **1973**, *8*, 319−331.

(11) McNulty, P. B.; Karel, M. Factors affecting flavor release and uptake in O/W emulsions, 3. Scale-up model and emulsion studies. *J. Food Technol.* **1973**, *8*, 415−427.

(12) Harrison, M.; Hills, B. P.; Bakker, J.; Clothier, T. Mathematical model of flavor release from liquid emulsions. *J. Food Sci.* **1997**, *62*, 653−658.

(13) McClements, D. J. *Food Emulsions—Principles, Practices, and Techniques*, 2nd ed.; CRC Press: New York, 2004.

(14) Bakker, J.; Mela, D. J. Effect of emulsion structure on flavor release and taste perception. In *Flavor-Food Interactions*; McGorrin, R. J., Leland, J. V., Eds.; American Chemical Society: Washington, DC, 1996.

(15) Charles, M.; Lambert, S.; Brondeur, P.; Courthaudon, J.; Guichard, E. Influence of formulation and structure of an oil-in-water emulsion on flavor release. In *Flavor Release*; Roberts, D. D., Taylor, A. J., Eds.; American Chemical Society: Washington, DC, 2000; pp 342−355.

(16) Voilley, A.; Espinosa Diaz, M. A.; Druaux, C.; Landy, P. Flavor release from emulsions and complex media. In *Flavor Release*; Roberts, D. D., Taylor, A. J., Eds.; American Chemical Society: Washington, DC, 2000; pp 142−152.

(17) Philippe, E.; Seuvre, A. M.; Colas, B.; Langendorff, V.; Schippa, C.; Voilley, A. Behavior of flavor compounds in model food systems: A thermodynamic study. *J. Agric. Food Chem.* **2003**, *51*, 1393−1398.

(18) Seuvre, A. M.; Espinosa Diaz, M. A.; Voilley, A. Transfer of aroma compounds through lipidic-aqueous interface in a complex system. *J. Agric. Food Chem.* **2002**, *50*, 1106−1110.

(19) Landy, P.; Courthaudon, J.; Dubois, C.; Voilley, A. Effect of interface in model food emulsions on the volatility of aroma compounds. *J. Agric. Food Chem.* **1996**, *44*, 526−530.

(20) Meynier, A.; Garillon, A.; Lethuaut, L.; Genot, C. Partition of five aroma compounds between air and skim milk, anhydrous milk fat or full-fat cream. *Lait* **2003**, *83*, 223−235.

(21) Roberts, D. D.; Pollien, P. Relative influence of milk components on flavor compounds volatility. In *Flavor Release*; Roberts, D. D., Taylor, A. J., Eds.; American Chemical Society: Washington, DC, 2000; pp 321−332.

(22) O'Neill, T. E. Flavor binding by food proteins: An overview. In *Flavor-Food Interactions*; McGorrin, R. J., Mela, D. J., Eds.; American Chemical Society: Washington, DC, 1996; pp 58−74.

(23) Guichard, E. Interactions between flavor compounds and food ingredients and their influence on flavor perception. *Food Rev. Int.* **2002**, *18*, 49−70.

(24) Maier, H. G. Binding of volatile aroma substances to nutrients and foodstuffs. In *Proceedings of the International Symposium on Aroma Research*; Maarse, H., Groenen, P. J., Eds.; Pudoc: Wageningen, 1975; pp 143−157.

(25) Roberts, D. D.; Pollien, P.; Watzke, B. Experimental and modeling studies showing the effect of lipid type and level on flavor release from milk-based liquid emulsions. *J. Agric. Food Chem.* **2003**, *51*, 189−195.

(26) Dubois, C.; Sergent, M.; Voilley, A. Flavoring of complex media: a model cheese example. In *Flavor-Food Interactions*; McGorrin, R. J., Leland, J. V., Eds.; American Chemical Society: Washington, DC, 1998; pp 213−226.

(27) Carey, M. E.; Asquith, T.; Linforth, R. S. T.; Taylor, A. J. Modeling the partition of volatile aroma compounds from a cloud emulsion. *J. Agric. Food Chem.* **2002**, *50*, 1985−1990.

(28) Rabe, S.; Krings, U.; Berger, R. G. Influence of oil-in-water emulsion characteristics on initial dynamic flavour release. *J. Sci. Food Agric.* **2003**, *83*, 1124−1133.

(29) Cramp, G. L.; Docking, A. M.; Ghosh, S.; Coupland, J. N. On the stability of oil-in-water emulsions to freezing. *Food Hydrocolloids* **2004**, *18*, 899−905.

(30) Coupland, J. N. Crystallization in emulsions. *Curr. Opin. Colloid Interface Sci.* **2002**, *7*, 445−450.

(31) Weast, R. C., Ed. *Handbook of Chemistry and Physics*, 56th ed.; CRC Press: Cleveland, OH, 1975.
(32) Bronlund, J.; Paterson, T. Moisture sorption isotherms for crystalline, amorphous and predominantly crystalline lactose powders. *Int. Dairy J.* **2004**, *14*, 247−254.
(33) Mathlouthi, M.; Roge, B. Water vapour sorption isotherms and the caking of food powders. *Food Chem.* **2003**, *82*, 61−71.
(34) Lammert, A. M.; Schmidt, S. J.; Day, G. A. Water activity and solubility of trehalose. *Food Chem.* **1998**, *61*, 139−144.
(35) Bunjes, H.; Drechsler, M.; Koch, M. H. J.; Westesen, K. Incorporation of the model drug ubidecarenone into solid lipid nanoparticles. *Pharm. Res.* **2001**, *18*, 287−293.
(36) Westesen, K.; Bunjes, H.; Koch, M. H. J. Physicochemical characterization of lipid nanoparticles and evaluation of their drug loading capacity and sustained release potential. *J. Controlled Release* **1997**, *48*, 223−236.
(37) Muller, R. H.; Mader, K.; Gohla, S. Solid lipid nanoparticles (SLN) for controlled drug delivery−A review of the state of the art. *Eur. J. Pharm. Biopharm.* **2000**, *50*, 161−177.
(38) Ueno, S.; Hamada, Y.; Sato, K. Controlling polymorphic crystallization of *n*-alkane crystals in emulsion droplets through interfacial heterogeneous nucleation. *Cryst. Growth Des.* **2003**, *3*, 935−939.

Received for review September 13, 2005. Revised manuscript received December 13, 2005. Accepted December 26, 2005.

JF052262W